
Article:
Tahir, B.A., Bragg, C.M., Wild, J.M. et al. (5 more authors) (2017) Impact of field number and beam angle on functional image-guided lung cancer radiotherapy planning. Physics in Medicine and Biology, 62 (17). pp. 7114-7130. ISSN 0031-9155

https://doi.org/10.1088/1361-6560/aa8074

Title

Impact of field number and beam angle on functional image-guided lung cancer radiotherapy planning

Running Title

^{3}He MRI guided lung IMRT

Authors

Bilal A. Tahir PhD[1,2], Chris M. Bragg PhD[3], Jim M. Wild PhD[2], James A. Swinscoe MSc[1], Sarah E. Lawless MRCP[3], Kerry A. Hart MSc[1,3], Matthew Q. Hatton FRCP, FRCR[1,3], Rob H. Ireland PhD[1,2]

Academic Units of Clinical Oncology[1] and Radiology[2], The University of Sheffield, UK

Weston Park Hospital[3], Sheffield Teaching Hospitals NHS Trust, Sheffield, UK

Correspondence Address

Rob Ireland, Academic Unit of Clinical Oncology, The University of Sheffield, S10 2SJ, UK

Email: r.ireland@sheffield.ac.uk

Conflict of Interest Notification: None

Key words

IMRT, NSCLC, radiation therapy, lung avoidance, hyperpolarised helium-3 MRI

Abstract

Purpose: To investigate the effect of beam angles and field number on functionally-guided intensity modulated radiotherapy (IMRT) normal lung avoidance treatment plans that incorporate hyperpolarised helium-3 magnetic resonance imaging (^{3}He-MRI) ventilation data.

Methods and Materials: Eight non-small cell lung cancer (NSCLC) patients had pre-treatment ^{3}He-MRI that was registered to inspiration breath-hold radiotherapy planning computed tomography (CT). IMRT plans that minimised the volume of total lung receiving ≥ 20 Gy (V_{20}) were compared with plans that minimised ^{3}He-MRI defined functional lung receiving ≥ 20 Gy (fV_{20}). Coplanar IMRT plans using 5-field manually optimised beam angles and 9-field equidistant plans were also evaluated. For each pair of plans, the Wilcoxon signed ranks test was used to compare fV_{20} and the percentage of planning target volume (PTV) receiving 90% of the prescription dose (PTV_{90}).

Results: Incorporation of ^{3}He-MRI led to median reductions in fV_{20} of 1.3% (range: 0.2 - 9.3%; p = 0.04) and 0.2% (range: 0 to 4.1%; p = 0.012) for 5- and 9-field arrangements, respectively. There was no clinically significant difference in target coverage.

Conclusions: Functionally-guided IMRT plans incorporating hyperpolarised ^{3}He-MRI information can reduce the dose received by ventilated lung without comprising PTV coverage. The effect was greater for optimised beam angles rather than uniformly spaced fields.

1 Introduction

1.1 The rationale for functional lung avoidance treatment planning

Attempts to improve survival rates for lung cancer patients undergoing curative intent treatment have focused on novel drug combinations and radiation intensification (Bradley *et al* 2015). However, the clinical benefits of dose escalation may be improved by better identification and treatment of the frequently occurring co-morbidities that reduce pre-radiotherapy pulmonary function (Marks *et al* 1995, Seppenwoolde *et al* 2002, Hoover *et al* 2014) and currently limit dose escalation due to the significant likelihood of radiation induced lung injury (RILI) (Madani *et al* 2007, Robbins *et al* 2012, Palma *et al* 2013). Minimisation of RILI risk to healthy, well ventilated and perfused lung while maximising the tumour dose is, therefore, a critical balancing act when planning radiation treatment.

Pulmonary function tests of the whole lung lack sensitivity to chronic disease (Simon *et al* 2012) and fail to provide the regional information required for functional dose optimisation when treatment planning (Marks *et al* 1993, 1997), whereas 3D imaging of regional pulmonary function can deliver the necessary localisation of healthy and defective tissue and aid with the assessment of pulmonary co-morbidity. Although single photon emission computed tomography (SPECT) has been the most commonly investigated modality for assessing such normal lung avoidance treatment planning, alternative techniques using magnetic resonance imaging (MRI) and CT have also received considerable attention (Ireland *et al* 2016).

1.2 Lung avoidance planning with SPECT

Initial work using functional data provided by 99mTc-labeled macroaggregated albumin perfusion SPECT, in a study of 56 lung cancer patients, demonstrated that functionally adapted radiation treatment planning was most useful for cases with small tumours and poor pulmonary function (Marks *et al* 1995). In a later study of 104 lung patients, by the same group at the Duke University Medical School, North Carolina, USA, 11% were found to have conventional treatment plans modified by inclusion of SPECT data to allow avoidance of functioning lung. These patients had extremely poor pre-radiotherapy pulmonary function and inhomogeneous perfusion maps (Munley *et al* 1999).

Others have demonstrated the feasibility of SPECT-guided conformal treatment planning but with smaller patient numbers (Cattaneo *et al* 1999). In a study of 6 patients, who were representative of

common perfusion defects identified from a study of 116 lung patients at The Netherlands Cancer Institute, Amsterdam, functional data only improved an automatic beam weight optimised conformal (3D-CRT) treatment plan for a single patient with a very large perfusion defect while there were no changes in planning parameters for those with smaller defects (Seppenwoolde *et al* 2002). Radiation was found to only affect small regions of lung when treating small tumours, therefore the improvement that could be gained by perfusion-weighted dose optimisation was less significant (Seppenwoolde *et al* 2002). In a related study conducted at The Royal Marsden, Sutton, UK, functional SPECT 3D-CRT planning similarly resulted in only one patient with large perfusion defects gaining benefit from the functional conformal plan while five with inhomogeneous perfusion did not. No additional benefit was gained by using non-coplanar fields (Christian *et al* 2005).

Further testing of the concept of functionally constrained dose planning became possible with the introduction of intensity-modulated radiotherapy (IMRT), since IMRT optimisation must take into account the dose distribution in healthy tissue as well as tumours (Bentzen 2005). The Duke University team demonstrated in one patient the potential to adapt IMRT planning constraints with functional SPECT data to divert dose from high to low perfused regions (Das *et al* 2004). In further studies at Duke University for 5 patients, IMRT plans were compared with and without SPECT guidance and functional V20 reduced by an absolute median of 5.2% with 9 beams (McGuire *et al* 2006) and 6.1% with 4 beams (McGuire *et al* 2010). 9 field IMRT was also used to produce a significant median reduction in functional V20 (the volume of lung receiving ≥ 20 Gy) of 6.8% for a group of 16 advanced stage patients at M.D. Anderson Cancer Center, Houston, TX, USA, with the degree of reduction tending to be greater in patients with a larger perfusion defect than those who had no or small perfusion defect (Shioyama *et al* 2007). In a separate study at the Royal Marsden, UK, 5 field IMRT and 4 field conformal plans were compared for 17 and 25 patients with no difference for early stage patients and significant improvements for stage III patients (Lavrenkov *et al* 2007, 2009). Another comparison of 3D conformal planning and IMRT found no advantage for either method but inclusion of perfusion SPECT in IMRT demonstrated a 3.2% absolute difference in functional V20 from a cohort of 10 patients in Jinan, China (Yin *et al* 2009). 3 beam IMRT and ventilation SPECT data was applied to 10 stage III patients in Ontario, Canada, and was considered beneficial when well ventilated lung did not surround the planning target volume (PTV) (Munawar *et al* 2010). A separate Canadian study in Quebec observed small but statistically significant changes (median 0.9 Gy) to mean perfusion-weighted lung dose when comparing anatomical and functional plans for 15 advanced stage patients but no significant difference was evident for functional V20 (St-Hilaire *et al* 2011). More recently, researchers from Jinan, China, constrained 7 field IMRT plans with

SPECT perfusion data to give a significant absolute functional V20 reduction of 3.1% from 10 stage I-III patients (Tian *et al* 2014).

1.3 Lung avoidance planning with MRI

Following the work of Lawrence Marks and others using SPECT for functional lung avoidance planning, Ireland and colleagues at The University of Sheffield, UK, explored the feasibility of using inert gas MRI for treatment planning (Ireland *et al* 2007) due to its superior spatial and temporal resolution (van Beek *et al* 2004, Stavngaard *et al* 2005). The incorporation of functional regions defined from ^{3}He MRI images into 5 or 7 beam IMRT plans for 6 stage I-III lung cancer patients produced a statistically significant 3.1% median reduction of functional V20. However, without large study numbers it is difficult to assess which groups of patients may benefit from lung avoidance functional planning. Therefore, a follow-on study in Sheffield investigated seven simulated scenarios that represented cases of non-small-cell lung cancer (NSCLC) with significant functional lung defects. Small but statistically significant reductions in functional V20 (median 2.7%) and mean functional lung dose (median 0.4 Gy) were possible when 5 field IMRT planning was supplemented by functional information (Bates *et al* 2009).

Other hyperpolarised gas MRI research centres have also begun investigations into functionally weighted radiotherapy lung planning. At the University of Wisconsin, Madison, USA, data from separate patients who had undergone inert gas MRI and planning CT was used in a single test case to demonstrate the feasibility of creating a helical Tomotherapy plan constrained using ventilated volumes defined by hyperpolarised ^{3}He MRI (Hodge *et al* 2010). Helical Tomotherapy planning was also explored by Cai et al at the University of Virginia, Charlottesville, USA, who simulated tumour volumes within the CTs of 6 patients (Cai *et al* 2011) and found a statistically significant 1.9% mean reduction in functional V20 and 0.8 Gy for mean functional lung dose. Although treatment plans themselves were not altered in a related study on the use of hyperpolarised ^{3}He MRI by a group in Massachusetts, USA, many issues such as patient setup, post-treatment ventilation changes and the potential for modifying treatment based on functional data are illustrated by 5 case studies (Allen *et al* 2011). In a study of 15 lung patients at the University of Western Ontario, London, Canada , ^{3}He MRI identified more cases of pre-existing chronic obstructive pulmonary disease (COPD) than previously diagnosed by CT and pulmonary function tests (Mathew *et al* 2012), which may affect choice of treatment as well as providing data for functionally-guided planning.

1.4 Lung avoidance planning with CT-based surrogate measurements of function

To avoid the use of SPECT or MRI, methods to derive surrogate functional lung parameters from either 4D-CT or breath-hold inhalation and exhalation CT images have been proposed (Guerrero *et al* 2005, 2006, Simon *et al* 2012). The feasibility of including this CT-based 'ventilation' or tissue expansion data into treatment planning has been explored by several groups. An initial study at M.D. Anderson Cancer Center, Houston, TX, USA, evaluated the impact of intensity based 4D-CT derived ventilation data on 9 beam IMRT plans for 21 stage III lung cancer patients. Although there was no significant difference in functional V20, a mean 2.9 Gy reduction in dose to functional lung was detected using a 90% threshold for functional tissue definition (Yaremko *et al* 2007).

The Jacobian CT derived metric of regional volume change was used in a study at Stanford University to show statistically significant reductions in mean dose to functional lung of 1.8 Gy for 6 field IMRT and 2.0 Gy for volumetric modulated arc therapy (VMAT) for 15 stage I-III patients (Yamamoto *et al* 2011).

In a related study, an alternative method of using 4D-CT data to functionally constrain VMAT and IMRT plans was attempted with 8 lung cancer patients with COPD at Hiroshima University, Japan (Kimura *et al* 2012). Application of a threshold of -860 HU defined a 'low attenuation area' (LAA) significantly reduced the V20 in functional plans compared with anatomical only plans (mean 1.5% for IMRT and mean 1.6% for VMAT) and produced a small but significant reduction in MLD (mean 0.23 Gy for IMRT, mean 0.5 Gy for VMAT).

Huang et al at the China Medical University Hospital, Taiwan, used a ΔV 'brute force geometric' method to calculate the surrogate measure of ventilation from 4D-CT (Huang *et al* 2013). Applying the method to 11 IMRT plans for stage III patients produced significant reductions of 1.2 Gy for mean functional lung dose and 2.6% for functional V20 by modifying gantry angles in the functional plans to avoid the highly functional regions.

1.5 Impact of beam angle and number on lung avoidance treatment planning

It is important to consider if beam orientation may have an effect on whether the inclusion of functional volumes has a significant impact on planning. For example, in a study of 16 stage III-IV lung cancer patients at Guangzhou Medical University, China, the inclusion of a Jacobian measure of function derived from 4D-CT into plans with 5 equally spaced beams resulted in a statistically significant mean reduction of 5.2% for functional V20. However, when beams angles were optimised there was no longer a significant difference between anatomical and functional plans (Wang *et al* 2014).

The impact of 4D-CT derived Jacobian data on lung avoidance, for 11 patients with small tumour volumes who were eligible for stereotactic ablative radiotherapy (SABR), was investigated at Tohoku University, Sendai, Japan (Kadoya *et al* 2015). Conformal treatment with 7-9 beams that were automatically determined by beam angle optimisation gave a 3.2% reduction (not statistically significant, t test, p=0.093) in functional V20 when a 90% thresholded functional region was used during planning.

In a comprehensive study to compare IMRT plans generated by inclusion of CT ventilation and SPECT ventilation data, Kida et al used 9 equally spaced beams and varied only the lung weight (importance) factor map (Kida *et al* 2016). A selection of 8 patients was taken from a larger 18 patient study that had shown low correlation between spatial overlap of defects seen on CT and SPECT ventilation images (Yamamoto *et al* 2014) and the correlation between the CT and SPECT weight factor maps was similarly low. Several patients showed little difference between the functional image-based and anatomic image-based plans, a common feature of several previous functional lung avoidance studies (Seppenwoolde *et al* 2002, Christian *et al* 2005).

Greater knowledge of the impact of beam arrangement and field number would be beneficial when incorporating functional information into treatment planning. Therefore, the aim of this study was, for the first time, to use ventilation data from ^{3}He-MRI to investigate the impact of beam arrangement for functionally-guided lung avoidance IMRT plans.

2 Methods and Materials

2.1 Patient characteristics

Ten NSCLC patients due to undergo radical radiotherapy were recruited to a research ethics committee approved prospective study. Patients gave written informed consent to undergo inspiration breath-hold CT and ^{3}He-MRI prior to treatment.

2.2 Image acquisition and registration

Inspiration breath-hold CT scans were acquired at 512 × 512 pixels with 2.5 mm slice thickness and 0.98 mm pixel size (GE Healthcare, Princeton, NJ, USA). Images were acquired while patients were in the conventional supine position with arms raised above the head. Patients performed a 530 ms

breath-hold via a room air filled 1L Tedlar bag (Jensen Inert Products, Coral Springs, FL, USA) to replicate the subsequent functional lung imaging procedure.

On the same day, patients underwent hyperpolarised ^{3}He-MR ventilation imaging on a 1.5 T whole body Eclipse scanner (Philips Medical Systems, Cleveland, OH, USA), fitted with a transmit-receive coil tuned to 48.5 MHz and an additional radiofrequency amplifier (2 kW, Analogic Corporation, Peabody, MA, USA). A volume coil (De Zanche *et al* 2008) allowed ^{3}He-MR images to be obtained in the treatment position, which is supine with arms up. A 3D gradient echo pulse sequence was employed (Wild *et al* 2005). Patients were imaged during a 16s inspiration breath-hold upon inhalation from a 1L Tedlar bag consisting of a mixture of equal amounts of ^{3}He gas (Spectra Gases, Huntingdon, UK) and N_2. Spin exchange optical pumping was used to hyperpolarize the ^{3}He gas to 30% (GE Healthcare, Princeton, NJ, USA).

The ^{3}He-MR and inspiration CT images were then imported into the Eclipse treatment planning system (TPS) (Varian Medical Systems, Palo Alto, CA, USA) for registration via the rigid control point tool (Ireland *et al* 2008, Tahir *et al* 2014).

2.3 Target volume definition

The breath-hold CT images were contoured in the Eclipse TPS. A gross tumour volume (GTV) was delineated for each patient. As per local protocol, a uniform margin of 5 mm was then added to the GTV to create the clinical target volume (CTV). This was further expanded by 15 mm craniocaudally and 10 mm axially to produce the planning target volume (PTV). The PTV of one the patients partially intersected with the spinal cord and thus the CTV-to-PTV margin was modified to 5 mm in that region. In addition, whole lung, spinal cord, oesophagus and heart structures were contoured. A normal tissue avoidance structure was defined by subtracting the PTV from the external body contour. Functional lung was segmented using a threshold defined as the mean plus three standard deviations of the background values of the ^{3}He-MR images.

2.4 IMRT Planning

Inverse planning was performed using the Dose-Volume-Optimiser module of the Eclipse TPS. The final forward dose calculation was performed using Eclipse's Anisotropic Analytic Algorithm (AAA) which accounts for lateral scatter and inhomogeneities (Bragg *et al* 2008). The dose and fractionation scheme employed was based on continuous hyperfractionated accelerated radiotherapy (CHART), which is 54 Gy in 36 fractions (Saunders *et al* 1997).

For each patient, four dynamic IMRT plans using coplanar 6 MV beams were generated with the aim of minimising the volume of either total lung receiving ≥ 20 Gy (V_{20}) or functional lung receiving ≥ 20 Gy (fV_{20}). Two of the four plans were designed with 5-fields, with beam angles manually optimised. For clinical acceptability, each plan was designed to meet the dosimetric requirements described in Table 1. Plans were then optimised by interactively adjusting constraints and objectives during inverse planning with relative priorities in the following order; maximizing target coverage, minimizing spinal cord dose, reducing dose to total or functional lung and limiting normal tissue dose (Bates *et al* 2009). To remove the subjectivity in beam angle optimisation, this process was repeated

Table 1. Intensity-modulated radiotherapy (IMRT) planning requirements.

PTV	Mean dose 54 Gy; 95% of PTV receiving at least 90% of the prescribed dose
TL or FL	Volume receiving ≥ 20 Gy no more than 35%
Spinal cord	Maximum dose ≤ 44 Gy
Oesophagus	Volume receiving ≥ 55 Gy no more than 35%
Heart	Volume receiving ≥ 45 Gy no more than 50%
Normal tissue	Maximum dose ≤ 60 Gy

Abbreviations. PTV, planning target volume; TL, total lung; FL, functional lung.

for two equidistant 9-field plans (Shioyama *et al* 2007). All plans were normalised such that the mean dose received by the PTV was 54 Gy. No patients were treated with the IMRT plans.

2.5 Plan evaluation

Plans were evaluated by the following dosimetric parameters:

- V_{10} (percentage of total lung receiving ≥ 10 Gy)
- fV_{10} (percentage of functional lung receiving ≥ 10 Gy)
- V_{20} (percentage of total lung receiving ≥ 20 Gy)
- fV_{20} (percentage of functional lung receiving ≥ 20 Gy)
- MLD (mean total lung dose in Gy)
- *f*MLD (mean functional lung dose in Gy)
- PTV_{90} (the percent PTV volume receiving 90% of the prescription dose).

To determine the best plan, a plan quality index defined as the ratio of PTV_{90}:fV_{20} was used where a higher value may permit dose escalation to the tumour while sparing of functional lung (Lavrenkov

et al 2007). In addition, the total number of monitor units (MUs) generated by each plan was recorded.

2.6 Statistical analysis

Statistical significance ($p < 0.05$) of differences between the four plans was assessed by the Wilcoxon signed rank test. Statistical analysis was performed using SPSS version 15.0 for Windows (SPSS, Chicago, IL, USA).

3 Results

3.1 Patient characteristics

Seven male and three female NSCLC patients (median age 75, range 58-80 years) underwent ^{3}He-MRI and breath-hold CT prior to radiotherapy. One patient had insufficient intake of ^{3}He gas to produce a viable ventilation image and for one patient, radical radiotherapy was not possible due to an excessively large PTV. Therefore, image data from eight patients was available for treatment planning evaluation (Table 2). As defined by the ^{3}He-MRI, the median functional lung as a percentage of total lung was 77% (range 65-95%). Representative registered CT and ^{3}He-MR images are shown in Figure 1.

Table 2. Non-small cell lung cancer patient characteristics.

Patient	Stage	Tumour Location	PTV Volume (cm^3)	Total Lung Volume (cm^3)	Functional Lung Volume (cm^3)	Functional Lung (as % of Total lung)
1	T_4N_0	Left upper lobe	769.6	4569.2	3270.5	71.6
2	T_2N_2	Left upper lobe	543.5	5409.1	3677.9	68.0
3	T_3N_1	Left lower lobe	308.7	4309.0	3850.9	89.4
4	T_4Nx	Left mid-upper lobe	830.3	8461.9	5459.7	64.5
5	T_2N_0	Left upper lobe	204.0	4219.0	4008.6	95.0
6	T_1N_0	Left mid lung	76.5	5117.4	3990.1	78.0
7	T_2N_1	Left upper lobe	1128.5	4481.0	3748.5	83.7
8	T_2N_0	Right mid lung	362.6	4730.1	3571.9	75.5

3.2 Plan evaluation

The functional lung, normal lung and PTV dose-volume histograms for the 5- and 9-field anatomically- and functionally-guided plans are displayed in Figure 2 for patient 2. Dosimetric parameters for all patients for the 5- and 9-field anatomically- and functionally-guided plans are displayed in Tables 3 and 4, respectively. To test whether 5 beams with manual beam angle optimisation could provide dosimetrically favourable plans to 9 equidistant beams, the plans that incorporated functional information for both are compared in Table 5. For the anatomical 9-field plan, the V_{20} of patient 7 was 35.7% and thus exceeded the planning constraint of 35%. Apart from this, all planning objectives and constraints pertaining to target coverage and critical structures were met.

For the 5-field plans, the median reduction in fV_{20} and *f*MLD when incorporating functional information was 1.3% (range: -0.2 to 9.3%; p = 0.04) and 0.2 Gy (range: 0 to 1.3 Gy; p = 0.03), respectively. For the 9-field arrangements, the median reduction of these parameters was 0.2% (range: 0 to 4.1%; p = 0.012) and 0.1 Gy (range: 0 to 0.3 Gy; p = 0.012), respectively. Comparing these parameters between the 5- and 9-field plans which incorporated functional information, the median differences between them were 2.7% (range: -5.7 to 5.2%; p = 0.263) and 1.3 Gy (range: -2.3 to 3.5 Gy; p = 0.161), respectively, both in favour of 5 fields.

Although there was no statistically significant difference in the PTV_{90} between the two 5-field plans, a marginal difference was observed between the two 9-field plans (0.1%; range: 0 to 0.9%; p = 0.012) but was not considered to be clinically significant. A larger difference in PTV_{90} was demonstrated between the 5- and 9-field functionally-guided plans, in favour of 9-fields (0.9%; range: 0.2 to 2.5%; p = 0.012). Comparison of the plan quality index between the 5- and 9-field functional plans demonstrated no significant difference. However, a greater total number of MUs were generated by the 9-field plans (median 627 MUs, range 473 - 1245 vs. 590 MUs, range 369 - 806; p = 0.036).

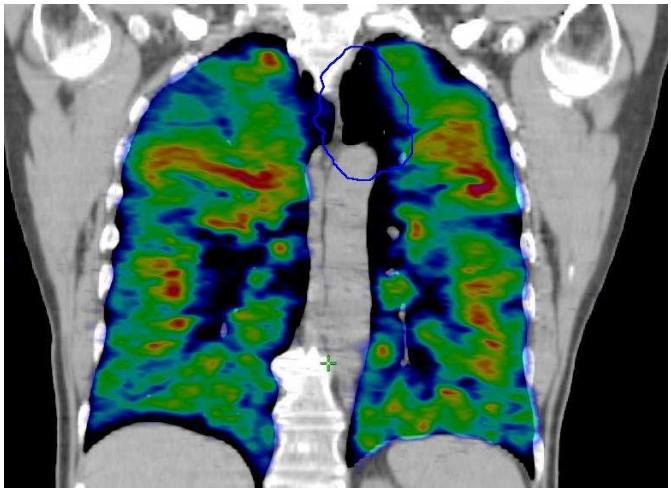

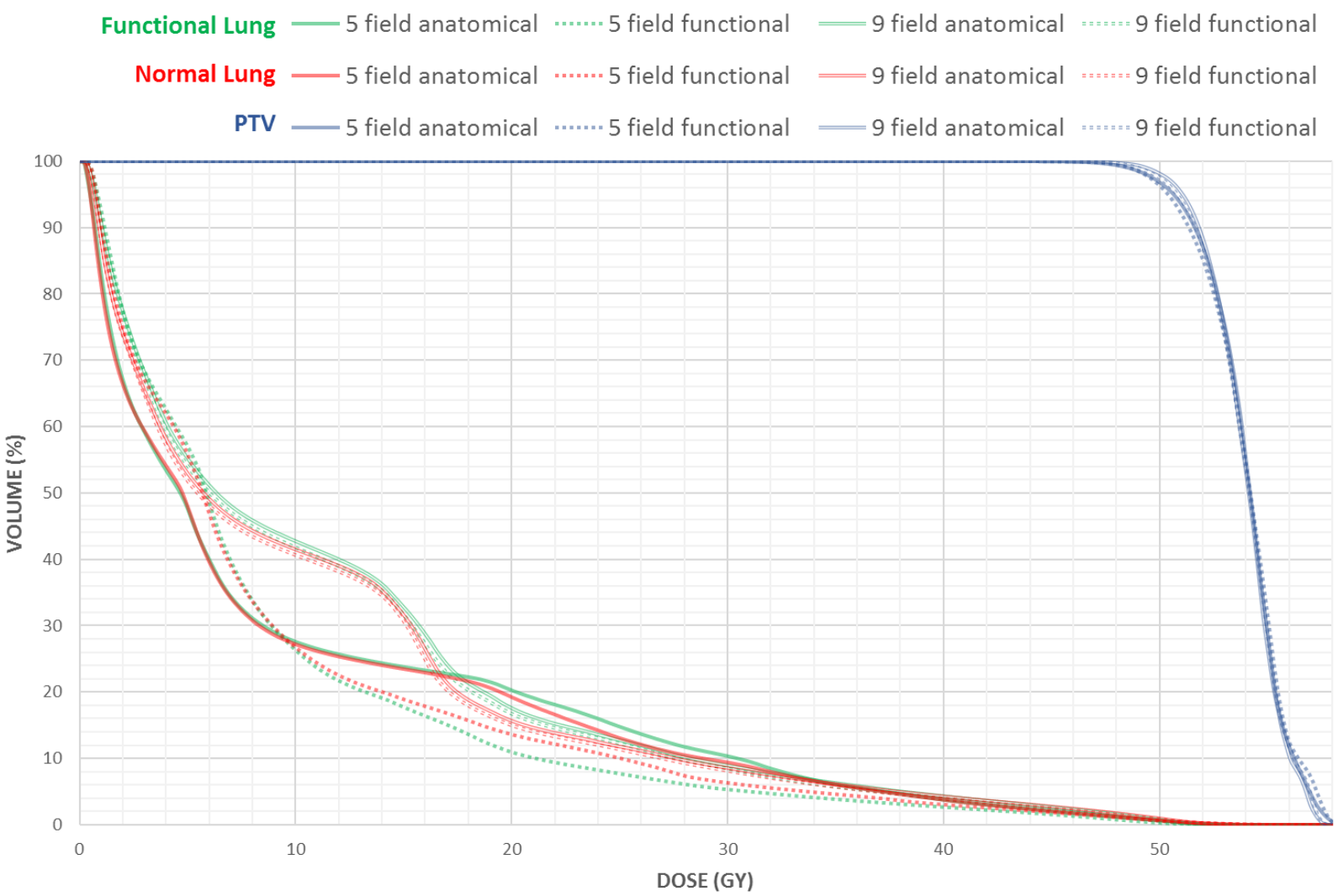

Figure 2. The functional lung (green), normal lung (red) and PTV (blue) dose-volume histograms for the 5- and 9-field anatomically- and functionally-guided plans for patient 2. Compared with the 5-field anatomically guided plan, the 5-field functionally guided plan, exhibits marked functional lung sparing with no detriment to PTV coverage. Conversely, the 9-field functionally guided exhibits only marginal functional lung sparing compared with its anatomically guided counterpart.

Table 3. Comparison of dose/volume parameters for 5-field anatomically (A) and functionally (B) guided IMRT plans.

Patient	V_{10}		fV_{10}		V_{20}		fV_{20}		MLD		*f*MLD		PTV_{90}		PTV_{90}:fV_{20}	
	A	B	A	B	A	B	A	B	A	B	A	B	A	B	A	B
1	28.8	28.4	25.6	25.5	11.7	11.4	11.4	11.1	8.2	8.0	8.1	7.9	99.7	99.6	8.8	9.0
2	28.6	29.7	29.0	29.5	19.2	13.6	20.3	11.0	9.6	9.2	9.8	8.8	99.0	99.0	4.9	9.0
3	42.1	42.1	43.3	43.3	21.4	21.5	21.3	21.2	11.5	11.5	11.5	11.5	98.3	98.3	4.6	4.6
4	21.1	21.2	25.9	25.9	11.7	11.1	13.5	11.1	7.3	7.2	8.5	8.4	96.9	96.0	7.2	8.7
5	15.6	15.7	15.6	15.8	7.9	8.2	7.9	8.1	5.1	5.2	5.1	5.1	96.5	97.0	12.2	12.0
6	10.8	10.7	10.1	9.9	5.3	5.2	4.5	4.4	4.5	4.5	4.1	4.1	97.6	97.7	21.7	22.2
7	49.5	43.9	46.0	40.4	31.2	26.2	27.9	23.5	14.1	12.8	13.2	11.9	99.1	97.4	3.6	4.2
8	19.4	20.6	21.5	21.7	11.3	9.3	13.0	10.1	7.6	7.4	8.1	7.6	97.1	95.1	7.5	9.4
Median difference	-0.02		0.03		0.45		1.33		0.15		0.16		0.05		-0.55	
Wilcoxon *p*	0.89		0.78		0.05		0.04		0.04		0.03		0.33		0.04	

Abbreviations: V_{10} (percentage of total lung receiving ≥ 10 Gy; fV_{10} (percentage of functional lung receiving ≥ 10 Gy; V_{20} (percentage of total lung receiving ≥ 20 Gy; fV_{20} (percentage of functional lung receiving ≥ 20 Gy; MLD (mean total lung dose in Gy); *f*MLD (mean functional lung dose in Gy); PTV_{90} (the percent PTV volume receiving 90% of the prescription dose).

Table 4. Comparison of dose/volume parameters for 9-field anatomically (C) and functionally (D) guided IMRT plans.

Patient	V_{10}		fV_{10}		V_{20}		fV_{20}		MLD		*f*MLD		PTV_{90}		PTV_{90}:fV_{20}	
	C	D	C	D	C	D	C	D	C	D	C	D	C	D	C	D
1	39.0	38.3	37.7	37.3	17.3	15.9	18.0	16.2	10.1	9.9	9.9	9.7	99.8	99.7	5.6	6.2
2	41.5	40.6	42.7	41.8	15.7	15.0	17.6	16.7	11.0	10.7	11.5	11.1	99.6	99.4	5.7	6.0
3	50.6	50.6	51.6	51.6	17.8	17.7	17.7	17.5	12.0	12.0	12.1	12.0	98.8	98.5	5.6	5.6
4	19.6	19.6	18.2	18.1	6.4	6.4	5.8	5.8	5.4	5.4	4.9	4.9	98.5	98.4	16.9	16.9
5	22.6	22.6	22.9	22.8	9.0	9.0	8.9	8.9	5.8	5.8	5.8	5.8	98.2	98.1	11.0	11.1
6	19.6	19.6	18.2	18.1	6.4	6.4	5.8	5.8	5.4	5.4	4.9	4.9	98.4	98.4	16.8	16.9
7	51.5	50.6	48.3	47.6	35.7	31.5	32.0	27.9	15.0	14.6	14.1	13.7	99.5	98.7	3.1	3.5
8	35.0	34.8	35.3	35.2	12.7	12.6	14.4	14.2	9.3	9.2	9.5	9.5	97.7	97.5	6.8	6.9
Median Difference	0.16		0.12		0.12		0.19		0.03		0.06		0.10		-0.07	
Wilcoxon *p*	0.04		0.01		0.03		0.01		0.07		0.01		0.01		0.01	

Table 5

Summary of dose/volume parameters for 5-field (B) - 9-field (D) functionally guided IMRT

	V_{10}	fV_{10}	V_{20}	fV_{20}	MLD	*f*MLD	PTV_{90}	PTV_{90}:fV_{20}
Median Difference	-8.68	-8.24	-1.28	-2.73	-1.19	-1.32	-0.92	1.72
Wilcoxon *p*	0.02	0.04	0.40	0.26	0.09	0.16	0.01	0.33

4 Discussion

4.1 IMRT planning

This study compared manually optimised 5-field IMRT plans and fixed equidistant 9-field arrangements, both with and without the incorporation of functional information defined by ^{3}He-MRI. Although the use of fewer fields are often preferred in clinical practice (Liu *et al* 2006), 9-field equidistant plans were also designed to remove subjectivity in selection of beam angles (Shioyama *et al* 2007) in order to investigate how effective the inverse planning algorithm is at avoiding functional lung.

When explicitly accounting for functional lung, a statistically significant median reduction in fV_{20} was demonstrated for the 5-field manually optimised plans (1.3%; p = 0.04). In contrast, only a modest reduction was observed for 9-fields (0.2%; p = 0.012). This suggests that beam angle optimisation is a more important factor than the inverse planning algorithm, by itself, in reducing the dose to functional lung. This is consistent with related studies that have demonstrated improved sparing of critical structures using fewer fields, optimised according to the geometry of the target and critical structures, than with uniformly spaced beams (Stein *et al* 1997, Liu *et al* 2006, Popple *et al* 2007).

Significantly higher V_{10} values were observed for the 9-field plans which can be attributed to the increased "low-dose bath" effect (Plowman *et al* 2008), where low-dose regions are more spread out as a consequence of using a greater number of fields (Bragg *et al* 2002). This caveat could be clinically relevant as V_{10} may be a better predictor of radiation pneumonitis than V_{20} (Schallenkamp *et al* 2007), and is consistent with Popple *et al* (2007) who showed that fewer fields, generating less MUs, reduce the dose received by organs-at-risk (OARs) due to a decrease in multileaf collimator leakage and transmission (Popple *et al* 2007). This is also demonstrated by the reduction in MUs generated by 5- fields in the present study.

The V_{10} and V_{20} results differ with those reported by Liu *et al* (2006), who did not show any significant differences in V_{10} and V_{20} between 5-, 7- and 9-field IMRT plans (Liu *et al* 2006). This could be due to the use of the step-and-shoot technique which requires less MUs compared to the sliding window mode used in the current study. As a consequence, critical structures receive less indirect dose from inter- and intraleaf transmission (Jothybasu *et al* 2009).

For the functionally-guided plans, all OAR tolerances including the spinal cord, heart and oesophagus were met. In addition, improvements in the fV_{20} and fMLD were without detriment to the PTV coverage, suggesting that functionally-guided IMRT can achieve clinically acceptable plans while preferentially sparing functional lung. An improvement in PTV_{90} was observed for 9-fields over 5-fields (0.9%; p = 0.012). This is in keeping with previous investigations which demonstrate that an increased number of fields provide enhanced target volume coverage and homogeneity (Popple *et al* 2007). Stein *et al* (1997) found that conformity of prescription dose to the tumour increased with increasing field number but at the cost of increased dose received by OARs (Stein *et al* 1997). If functionally-guided IMRT was to be applied in practice, a clinical decision would need to be made whether small improvements such as 0.9% in conformity can outweigh the benefits of increased functional avoidance in addition to the reduction in manpower constraints when using fewer fields.

One disadvantage of using fewer fields was a greater occurrence of hot spots in normal tissue. In order to mitigate this effect, it was necessary to fine tune beam angles and edit the fluence of individual beams. This required more time to plan than the uniformly spaced 9-field plans which required only a single optimisation to produce acceptable plans. However, this additional time requirement for 5-fields could be dependent on the TPS and thus not necessarily true for other commercial systems.

The highest median reduction in fV_{20} of 1.3% is lower than that reported in several previous ^{3}He-MRI, SPECT and CT-based functionally-guided IMRT studies (McGuire *et al* 2006, Shioyama *et al* 2007, Ireland *et al* 2007, Bates *et al* 2009, Wang *et al* 2014, Yamamoto *et al* 2016). This may be due to the different methods used to segment the functional lung volume or other methodological differences (Ireland *et al* 2016). It has been suggested that a greater degree of functional defects will lead to larger reductions in fV_{20} (Seppenwoolde *et al* 2002, Bates *et al* 2009). In the present study, the largest individual reductions demonstrated were 2.4 – 9.3%, shown by patients 2, 4, 7 and 8. The location of ventilation defect in relation to target volume was an important factor in reducing fV_{20}. For example, patient 2, who had the largest reduction of fV20, had large functional defects in proximity to the target volume. In contrast, patient 1 had relatively large defects spanning across approximately 30% of the total lung while no significant reduction in fV_{20} was observed. When optimizing solely based on anatomical information for this patient, only a small proportion of functional lung was in the pathway of the beams and thus no significant differences were observed compared with the functionally-guided IMRT plan.

Although patients 3 and 4 did not show any significant differences between 9-field anatomically- and functionally-guided plans, it was perhaps surprising that reductions of 3.7 and 5.3% respectively in fV_{20} were observed when compared with the 5-field arrangement. Patient 3 had a large centrally located tumour and so more equally spaced beam angles would be preferred in this situation. In addition, each of the 5 fields would have a larger contribution to meeting the prescription dose and this could explain why 9-fields were able to achieve improvements in functional lung dose.

The clinical significance on patient outcome and long term survival will require further investigation but the goal of lung avoidance planning is in line with the aspiration to lower the non-cancerous lung dose as far as possible.

4.2 Study limitations

As with many other related studies, one limitation of this study is that it uses lung ventilation data alone. Both ventilation and perfusion would be preferable for the full assessment of lung function (Yuan *et al* 2011, Ireland *et al* 2016).

The inhalation CT images used in this study were acquired at functional residual capacity (FRC) + 1L in order to match the ^{3}He MRI breathing manoeuvre, which provides significant improvements in CT and ^{3}He MRI image registration (Ireland *et al* 2008) and improved lung sparing compared to expiration breath-hold (Tahir *et al* 2010). Therefore, the breathing manoeuvre may have led to some of the observed discrepancies from other studies. In addition, hyperpolarised gas MRI (Halaweish *et al* 2013) and CT ventilation (Mistry *et al* 2013) have been shown to be sensitive to inflation state. Due to limited temporal resolution, the majority of previous nuclear medicine based studies employed tidal breathing acquisitions for functional image acquisition. The differences in breathing manoeuvre would inevitably give rise to differences in defect volumes and dosimetric parameters compared with the present study.

5 Conclusion

Functionally-guided IMRT plans incorporating hyperpolarised ^{3}He-MRI information accurately registered to inspiration CT can reduce the dose received by ventilated lung without comprising tumour coverage. The selection of optimal beam angles can have a greater impact on these differences than uniformly spaced field arrangements.

Acknowledgements

This article presents independent research funded by Sheffield Hospitals Charity, Weston Park Hospital Charity, Yorkshire Cancer Research, The University of Sheffield James Morrison Fund, EPSRC and the National Institute of Health Research (NIHR). The views expressed are those of the authors and not necessarily those of the NHS, the funders or the Department of Health. We also thank Emma Bates, Patricia Fisher, Bernadette Foran, Jayaram Mohanamurali, Gillian Brown, Neil Woodhouse, Cath Billings, Jan Johnson and Helen Simpson for their assistance and are grateful for the loan of the ^{3}He gas polarizer from GE Healthcare and support from Philips Medical Systems.

References

Allen A M, Albert M, Caglar H B, Zygmanski P, Soto R, Killoran J and Sun Y 2011 Can hyperpolarized helium MRI add to radiation planning and follow-up in lung cancer? *J. Appl. Clin. Med. Phys.* **12** 3357

Bates E L, Bragg C M, Wild J M, Hatton M Q and Ireland R H 2009 Functional image-based radiotherapy planning for non-small cell lung cancer: A simulation study *Radiother. Oncol.* **93** 32–6

van Beek E J R, Wild J M, Kauczor H U, Schreiber W, Mugler J P and De Lange E E 2004 Functional MRI of the lung using hyperpolarized 3-helium gas *J. Magn. Reson. Imaging* **20** 540–54

Bentzen S M 2005 Theragnostic imaging for radiation oncology: Dose-painting by numbers *Lancet Oncol.* **6** 112–7

Bradley J D, Paulus R, Komaki R, Masters G, Blumenschein G, Schild S, Bogart J, Hu C, Forster K, Magliocco A, Kavadi V, Garces Y I, Narayan S, Iyengar P, Robinson C, Wynn R B, Koprowski C, Meng J, Beitler J, Gaur R, Curran W and Choy H 2015 Standard-dose versus high-dose conformal radiotherapy with concurrent and consolidation carboplatin plus paclitaxel with or without cetuximab for patients with stage IIIA or IIIB non-small-cell lung cancer (RTOG 0617): a randomised, two-by-two factorial p *Lancet Oncol.* **16** 187–99

Bragg C M, Conway J and Robinson M H 2002 The role of intensity-modulated radiotherapy in the treatment of parotid tumors *Int. J. Radiat. Oncol. Biol. Phys.* **52** 729–38

Bragg C M, Wingate K and Conway J 2008 Clinical implications of the anisotropic analytical algorithm for IMRT treatment planning and verification *Radiother. Oncol.* **86** 276–84

Cai J, McLawhorn R, Altes T A, de Lange E, Read P W, Larner J M, Benedict S H and Sheng K 2011 Helical tomotherapy planning for lung cancer based on ventilation magnetic resonance imaging *Med. Dosim.* **36** 389–96

Cattaneo G, Rizzo G, Lombardi P, Ceresoli G, Savi A, Gilardi M, Villa E and Calandrino R 1999 Integration of computerized tomography imaging with single photon emission in a commercial system for developing radiotherapy fields: application to conformational irradiation for lung carcinoma *Radiol. Med.* **97** 272–8

Christian J A, Partridge M, Nioutsikou E, Cook G, McNair H A, Cronin B, Courbon F, Bedford J L and Brada M 2005 The incorporation of SPECT functional lung imaging into inverse radiotherapy planning for non-small cell lung cancer *Radiother. Oncol.* **77** 271–7

Das S K, Miften M M, Zhou S, Bell M, Munley M T, Whiddon C S, Craciunescu O, Baydush A H, Wong T, Rosenman J G, Dewhirst M W and Marks L B 2004 Feasibility of optimizing the dose distribution in lung tumors using fluorine-18-fluorodeoxyglucose positron emission tomography and single photon emission computed tomography guided dose prescriptions *Med. Phys.* **31** 1452–61

Guerrero T, Sanders K, Castillo E, Zhang Y, Bidaut L, Pan T and Komaki R 2006 Dynamic ventilation imaging from four-dimensional computed tomography *Phys. Med. Biol.* **51** 777–91

Guerrero T, Sanders K, Noyola-Martinez J, Castillo E, Zhang Y, Tapia R, Guerra R, Borghero Y and

Komaki R 2005 Quantification of regional ventilation from treatment planning CT *Int. J. Radiat. Oncol. Biol. Phys.* **62** 630–4

Halaweish A F, Hoffman E A, Thedens D R, Fuld M K, Sieren J P and van Beek E J R 2013 Effect of lung inflation level on hyperpolarized 3He apparent diffusion coefficient measurements in never-smokers. *Radiology* **268** 572–80

Hodge C W, Tomé W A, Fain S B, Bentzen S M and Mehta M P 2010 On the use of hyperpolarized helium MRI for conformal avoidance lung radiotherapy *Med. Dosim.* **35** 297–303

Hoover D A, Capaldi D P I, Sheikh K, Palma D A, Rodrigues G B, Dar A R, Yu E, Dingle B, Landis M, Kocha W, Sanatani M, Vincent M, Younus J, Kuruvilla S, Gaede S, Parraga G and Yaremko B P 2014 Functional lung avoidance for individualized radiotherapy (FLAIR): study protocol for a randomized, double-blind clinical trial *BMC Cancer* **14** 934

Huang T-C, Hsiao C-Y, Chien C-R, Liang J-A, Shih T-C and Zhang G G 2013 IMRT treatment plans and functional planning with functional lung imaging from 4D-CT for thoracic cancer patients. *Radiat. Oncol.* **8** 3

Ireland R H, Bragg C M, McJury M, Woodhouse N, Fichele S, van Beek E J R, Wild J M and Hatton M Q 2007 Feasibility of image registration and intensity-modulated radiotherapy planning with hyperpolarized helium-3 magnetic resonance imaging for non-small-cell lung cancer *Int. J. Radiat. Oncol. Biol. Phys.* **68** 273–81

Ireland R H, Tahir B A, Wild J M, Lee C E and Hatton M Q 2016 Functional image-guided radiotherapy planning for normal lung avoidance *Clin. Oncol.* **28** 695–707

Ireland R H, Woodhouse N, Hoggard N, Swinscoe J A, Foran B H, Hatton M Q and Wild J M 2008 An image acquisition and registration strategy for the fusion of hyperpolarized helium-3 MRI and x-ray CT images of the lung *Phys. Med. Biol.* **53** 6055–63

Jothybasu K S, Bahl A and V. Subramani, G. K. Rath, D. N. Sharma P K J 2009 Static versus dynamic intensity-modulated radiotherapy: Profile of integral dose in carcinoma of the nasopharynx *J. Med. Phys.* **34(2)** 66–72

Kadoya N, Cho S Y, Kanai T, Onozato Y, Ito K, Dobashi S, Yamamoto T, Umezawa R, Matsushita H, Takeda K and Jingu K 2015 Dosimetric impact of 4-dimensional computed tomography ventilation imaging-based functional treatment planning for stereotactic body radiation therapy with 3-dimensional conformal radiation therapy *Pract. Radiat. Oncol.* **5** e505–12

Kida S, Bal M, Kabus S, Negahdar M, Shan X, Loo B W, Keall P J and Yamamoto T 2016 CT ventilation functional image-based IMRT treatment plans are comparable to SPECT ventilation functional image-based plans *Radiother. Oncol.* **118** 521–7

Kimura T, Nishibuchi I, Murakami Y, Kenjo M, Kaneyasu Y and Nagata Y 2012 Functional image-guided radiotherapy planning in respiratory-gated intensity-modulated radiotherapy for lung cancer patients with chronic obstructive pulmonary disease *Int. J. Radiat. Oncol. Biol. Phys.* **82** e663–70

Lavrenkov K, Christian J A, Partridge M, Niotsikou E, Cook G, Parker M, Bedford J L and Brada M 2007 A potential to reduce pulmonary toxicity: the use of perfusion SPECT with IMRT for functional lung avoidance in radiotherapy of non-small cell lung cancer. *Radiother. Oncol.* **83** 156–62

Lavrenkov K, Singh S, Christian J A, Partridge M, Nioutsikou E, Cook G, Bedford J L and Brada M 2009 Effective avoidance of a functional SPECT-perfused lung using intensity modulated radiotherapy (IMRT) for non-small cell lung cancer (NSCLC): an update of a planning study. *Radiother. Oncol.* **91** 349–52

Liu H H, Jauregui M, Zhang X, Wang X, Dong L and Mohan R 2006 Beam angle optimization and reduction for intensity-modulated radiation therapy of non-small-cell lung cancers *Int. J. Radiat. Oncol. Biol. Phys.* **65** 561–72

Madani I, De Ruyck K, Goeminne H, De Neve W, Thierens H and Van Meerbeeck J 2007 Predicting risk of radiation-induced lung injury *J. Thorac. Oncol.* **2** 864–74

Marks L B, Munley M T, Spencer D P, Sherouse G W, Bentel G C, Hoppenworth J, Chew M, Jaszczak R J, Coleman R E and Prosnitz L R 1997 Quantification of radiation-induced regional lung injury

with perfusion imaging *Int. J. Radiat. Oncol. Biol. Phys.* **38** 399–409

Marks L B, Spencer D P, Bentel G C, Ray S K, Sherouse G W, Sontag M R, Edward Coleman R, Jaszczak R J, Turkington T G, Tapson V and Prosnitz L R 1993 The utility of SPECT lung perfusion scans in minimizing and assessing the physiologic consequences of thoracic irradiation *Int. J. Radiat. Oncol. Biol. Phys.* **26** 659–68

Marks L B, Spencer D P, Sherouse G W, Bentel G, Clough R, Vann K, Jaszczak R, Coleman R E and Prosnitz L R 1995 The role of three dimensional functional lung imaging in radiation treatment planning: the functional dose-volume histogram *Int. J. Radiat. Oncol. Biol. Phys.* **33** 65–75

Mathew L, Vandyk J, Etemad-Rezai R, Rodrigues G and Parraga G 2012 Hyperpolarized 3He pulmonary functional magnetic resonance imaging prior to radiation therapy *Med. Phys.* **39** 4284–90

McGuire S M, Marks L B, Yin F F and Das S K 2010 A methodology for selecting the beam arrangement to reduce the intensity-modulated radiation therapy (IMRT) dose to the SPECT-defined functioning lung *Phys. Med. Biol.* **55** 403–16

McGuire S M, Zhou S, Marks L B, Dewhirst M, Yin F F and Das S K 2006 A methodology for using SPECT to reduce intensity-modulated radiation therapy (IMRT) dose to functioning lung *Int. J. Radiat. Oncol. Biol. Phys.* **66** 1543–52

Mistry N N, Diwanji T, Shi X, Pokharel S, Feigenberg S, Scharf S M and D'Souza W D 2013 Evaluation of fractional regional ventilation using 4D-CT and effects of breathing maneuvers on ventilation *Int. J. Radiat. Oncol. Biol. Phys.* **87** 825–31

Munawar I, Yaremko B P, Craig J, Oliver M, Gaede S, Rodrigues G, Yu E, Reid R H, Leung E, Urbain J-L, Chen J and Wong E 2010 Intensity modulated radiotherapy of non-small-cell lung cancer incorporating SPECT ventilation imaging *Med. Phys.* **37** 1863–72

Munley M T, Marks L B, Scarfone C, Sibley G S, Patz Jr. E F, Turkington T G, Jaszczak R J, Gilland D R, Anscher M S and Coleman R E 1999 Multimodality nuclear medicine imaging in three-dimensional radiation treatment planning for lung cancer: challenges and prospects *Lung Cancer* **23** 105–14

Palma D A, Senan S, Tsujino K, Barriger R B, Rengan R, Moreno M, Bradley J D, Kim T H, Ramella S, Marks L B, De Petris L, Stitt L and Rodrigues G 2013 Predicting radiation pneumonitis after chemoradiation therapy for lung cancer: An international individual patient data meta-analysis *Int. J. Radiat. Oncol. Biol. Phys.* **85** 444–50

Plowman P N, Cooke K and Walsh N 2008 Indications for tomotherapy/intensity-modulated radiation therapy in paediatric radiotherapy: Extracranial disease *Br. J. Radiol.* **81** 872–80

Popple R A, Fiveash J B and Brezovich I A 2007 Effect of beam number on organ-at-risk sparing in dynamic multileaf collimator delivery of intensity modulated radiation therapy. *Med. Phys.* **34** 3752–9

Robbins M E, Brunso-Bechtold J K, Peiffer A M, Tsien C I, Bailey J E and Marks L B 2012 Imaging radiation-induced normal tissue injury *Radiat. Res.* **177** 449–66

Saunders M, Dische S, Barrett A, Harvey A, Gibson D and Parmar M 1997 Continuous hyperfractionated accelerated radiotherapy (CHART) versus conventional radiotherapy in non-small-cell lung cancer: A randomised multicentre trial *Lancet* **350** 161–5

Schallenkamp J M, Miller R C, Brinkmann D H, Foote T and Garces Y I 2007 Incidence of radiation pneumonitis after thoracic irradiation: Dose-volume correlates *Int. J. Radiat. Oncol. Biol. Phys.* **67** 410–6

Seppenwoolde Y, Engelsman M, De Jaeger K, Muller S H, Baas P, McShan D L, Fraass B a, Kessler M L, Belderbos J S a, Boersma L J and Lebesque J V 2002 Optimizing radiation treatment plans for lung cancer using lung perfusion information *Radiother. Oncol.* **63** 165–77

Shioyama Y, Jang S Y, Liu H H, Guerrero T, Wang X, Gayed I W, Erwin W D, Liao Z, Chang J Y, Jeter M, Yaremko B P, Borghero Y O, Cox J D, Komaki R and Mohan R 2007 Preserving functional lung using perfusion imaging and intensity-modulated radiation therapy for advanced-stage non-small cell lung cancer *Int. J. Radiat. Oncol. Biol. Phys.* **68** 1349–58

Simon B A, Kaczka D W, Bankier A A and Parraga G 2012 What can computed tomography and magnetic resonance imaging tell us about ventilation? *J. Appl. Physiol.* **113** 647–57

St-Hilaire J, Lavoie C, Dagnault A, Beaulieu F, Morin F, Beaulieu L and Tremblay D 2011 Functional avoidance of lung in plan optimization with an aperture-based inverse planning system *Radiother. Oncol.* **100** 390–5

Stavngaard T, Søgaard L V, Mortensen J, Hanson L G, Schmiedeskamp J, Berthelsen A K and Dirksen A 2005 Hyperpolarised 3He MRI and 81mKr SPECT in chronic obstructive pulmonary disease *Eur. J. Nucl. Med. Mol. Imaging* **32** 448–57

Stein J, Mohan R, Wang X H, Bortfeld T, Wu Q, Preiser K, Ling C C and Schlegel W 1997 Number and orientations of beams in intensity-modulated radiation treatments. *Med. Phys.* **24** 149–60

Tahir B A, Bragg C M, Lawless S E, Hatton M Q F and Ireland R H 2010 Dosimetric evaluation of inspiration and expiration breath-hold for intensity-modulated radiotherapy planning of non-small cell lung cancer *Phys. Med. Biol.* **55** N191-9

Tahir B A, Swift A J, Marshall H, Parra-Robles J, Hatton M Q, Hartley R, Kay R, Brightling C E, Vos W, Wild J M and Ireland R H 2014 A method for quantitative analysis of regional lung ventilation using deformable image registration of CT and hybrid hyperpolarized gas/1H MRI *Phys. Med. Biol.* **59** 7267–77

Tian Q, Zhang F, Wang Y and Qu W 2014 Impact of different beam directions on intensity-modulated radiation therapy dose delivered to functioning lung tissue identified using single-photon emission computed tomography *Wspolczesna Onkol.* **18** 438–43

Wang R, Zhang S, Yu H, Lin S, Zhang G, Tang R and Qi B 2014 Optimal beam arrangement for pulmonary ventilation image-guided intensity-modulated radiotherapy for lung cancer *Radiat. Oncol.* **9** 184

Wild J M, Fichele S, Woodhouse N, Paley M N J, Kasuboski L and Van Beek E J R 2005 3D volume-localized pO2 measurement in the human lung with 3He MRI *Magn. Reson. Med.* **53** 1055–64

Yamamoto T, Kabus S, Bal M, Keall P, Benedict S and Daly M 2016 The first patient treatment of computed tomography ventilation functional image-guided radiotherapy for lung cancer *Radiother. Oncol.* **118** 227–31

Yamamoto T, Kabus S, von Berg J, Lorenz C and Keall P J 2011 Impact of four-dimensional computed tomography pulmonary ventilation imaging-based functional avoidance for lung cancer radiotherapy *Int. J. Radiat. Oncol. Biol. Phys.* **79** 279–88

Yamamoto T, Kabus S, Lorenz C, Mittra E, Hong J C, Chung M, Eclov N, To J, Diehn M, Loo B W and Keall P J 2014 Pulmonary ventilation imaging based on 4-dimensional computed tomography: Comparison with pulmonary function tests and SPECT ventilation images *Int. J. Radiat. Oncol. Biol. Phys.* **90** 414–22

Yaremko B P, Guerrero T M, Noyola-Martinez J, Guerra R, Lege D G, Nguyen L T, Balter P A, Cox J D and Komaki R 2007 Reduction of normal lung irradiation in locally advanced non-small-cell lung cancer patients, using ventilation images for functional avoidance *Int. J. Radiat. Oncol. Biol. Phys.* **68** 562–71

Yin Y, Chen J, Li B, Liu T, Lu J, Bai T, Dong X and JM Y 2009 Protection of lung function by introducing single photon emission computed tomography lung perfusion image into radiotherapy plan of lung cancer *Chin. Med. J. (Engl).* **122** 509–13

Yuan S, Frey K A, Gross M D, Hayman J A, Arenberg D, Curtis J L, Cai X-W, Ramnath N, Kalemkerian G P, Ten Haken R K, Eisbruch A and Kong F-M 2011 Semiquantification and classification of local pulmonary function by V/Q single photon emission computed tomography in patients with non-small cell lung cancer: potential indication for radiotherapy planning *J. Thorac. Oncol.* **6** 71–8

De Zanche N, Chhina N, Teh K, Randell C, Pruessmann K P and Wild J M 2008 Asymmetric quadrature split birdcage coil for hyperpolarized 3He lung MRI at 1.5T *Magn. Reson. Med.* **60** 431–8